J. Phycol. *, ***–*** (2018)

DOI: 10.1111/jpy.12776

UNDER PRESSURE: BIOMECHANICAL LIMITATIONS OF DEVELOPING PNEUMATOCYSTS IN THE BULL KELP (*NEREOCYSTIS LUETKEANA*, PHAEOPHYCEAE)[1]

Lauran M. Liggan[2] *and Patrick T. Martone*

Department of Botany and Beaty Biodiversity Research Centre, University of British Columbia, Vancouver British Columbia, Canada V6T1Z4

Bamfield Marine Sciences Centre, 100 Pachena Road, Bamfield British Columbia, Canada V0R1B0

Maintaining buoyancy with gas-filled floats (pneumatocysts) is essential for some subtidal kelps to achieve an upright stature and compete for light . However, as these kelps grow up through the water column, pneumatocysts are exposed to substantial changes in hydrostatic pressure, which could cause complications as internal gases may expand or contract, potentially causing them to rupture, flood, and lose buoyancy. In this study, we investigate how pneumatocysts of *Nereocystis luetkeana* resist biomechanical stress and maintain buoyancy as they develop across a hydrostatic gradient. We measured internal pressure, material properties, and pneumatocyst geometry across a range of thallus sizes and collection depths to identify strategies used to resist pressure-induced mechanical failure. Contrary to expectations, all pneumatocysts had internal pressures less than atmospheric pressure, ensuring that thalli are always exposed to a positive pressure gradient and compressional loads, indicating that they are more likely to buckle than rupture at all depths. Small pneumatocysts collected from depths between 1 and 9 m (inner radius = 0.4–1.0 cm) were demonstrated to have elevated wall stresses under high compressive loads and are at greatest risk of buckling. Although small kelps do not adjust pneumatocyst material properties or geometry to reduce wall stress as they grow, they are ~3.4 times stronger than they need to be to resist hydrostatic buckling. When tested, pneumatocysts buckled around 35 m depth, which agrees with previous measures of lower limits due to light attenuation, suggesting that hydrostatic pressure may also define the lower limit of *Nereocystis* in the field.

Key index words: **buoyancy; depth zonation; development; gas bladder; hydrostatic pressure; macroalgae; modulus; stress**

***Abbreviations*: atm, atmosphere; ESF, environmental safety factor; *g*, gravitational acceleration; *h*, water depth; kPa, kilopascal; P_{atm}, atmospheric pressure; P_{gauge}, gauge pressure; P_i, internal pneumatocyst pressure; P_{mi}, initial manometer pressure; P_o, hydrostatic pressure; P_{Pn}, pneumatocyst pressure; r_i, internal pneumatocyst radius; r_o, outer pneumatocyst radius; *t*, pneumatocyst wall thickness; V_{mf}, total volume of the manometer and pneumatocyst; V_{mi}, initial manometer volume; V_{Pn}, pneumatocyst volume; ρ, density; σ_{avg}, average material stress; σ_{buckle}, buckling material stress**

The bull kelp *Nereocystis luetkeana* (hereafter *Nereocystis*) builds unique and naturally endemic three-dimensional habitats along the west coast of North America (Springer et al. 2007). Upright *Nereocystis* thalli are supported not by rigid stipes as in some other subtidal kelps, but by single gas-filled floats called pneumatocysts, which keep slender, flexible thalli upright in the water column to access light for photosynthesis and to avoid benthic herbivores (Koehl and Wainwright 1977, Johnson and Koehl 1994, Denny et al. 1997, Springer et al. 2007). Gas-filled structures are known from many seaweed species, especially within the brown algae (e.g., *Ascophyllum* spp., *Fucus* spp., *Sargassum* spp., *Durvillaea* spp.; Dromgoole 1981b, Brackenbury et al. 2006), however pneumatocysts produced by kelps (i.e., *N. luetkeana*, *Macrocystis pyrifera*, *Pelagophycus porra*) evolved independently from those of other macroalgae at least once (Thiel and Gutow 2005, Lane et al. 2006) and are developmentally distinct (Yoon et al. 2001, Lane et al. 2006, Charrier et al. 2012). Pneumatocysts of *Nereocystis* are particularly interesting because, unlike gas-filled floats in most other species, they inflate at depth and ascend through the water column toward the surface while experiencing a decreasing gradient of hydrostatic pressure (Fig. 1). The ability of *Nereocystis* pneumatocysts to resist breaking during their ascent is remarkable and worthy of further investigation.

Previous studies have shown that brown algae can resist mechanical forces as they develop by adjusting structural and mechanical properties to prevent organs (i.e., holdfast, stipe, blade, pneumatocyst) from breaking under extreme physical stress, such as wave forces or changes in hydrostatic pressure due to tidal fluctuations (Dromgoole 1981a,b,

[1]Received 6 December 2017. Accepted 16 July 2018. First Published Online 11 August 2018.
[2]Author for correspondence: e-mail liggan.l@gmail.com.
Editorial Responsibility: A. Buschmann (Associate Editor)

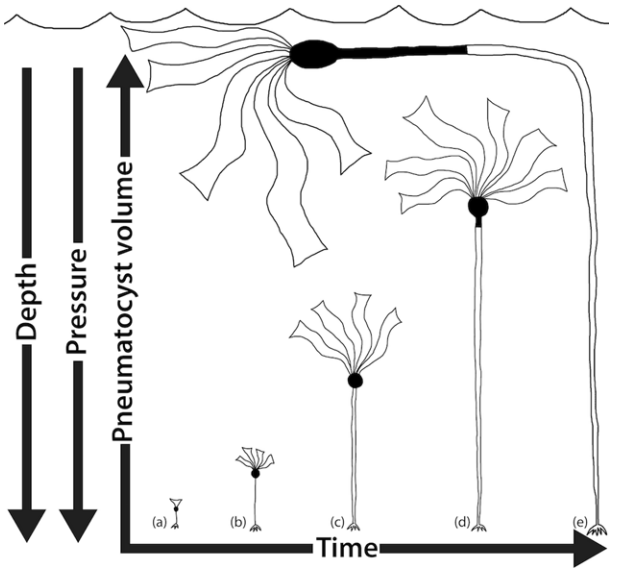

FIG. 1. Schematic of pneumatocyst development in growing *Nereocystis* thalli (pneumatocysts shaded black; arrows pointing toward increasing parameter values). (a) Young thalli develop small pneumatocysts subtidally, up to 35 m deep, where hydrostatic pressure is greatest during the life cycle. (b and c) Over time stipes elongate and pneumatocyst volume increases as pneumatocysts move toward the surface and experience less pressure. (d) As thalli grow pneumatocyst volume continues to increase and expands into the stipe. (e) Mature thalli have large pneumatocysts (more than 300 times their original size) that often reach the surface, experiencing only atmospheric (not hydrostatic) pressure.

Johnson and Koehl 1994, Utter and Denny 1996, Koehl 1999, Hale 2001, Harder et al. 2006, Starko and Martone 2016). In particular, pneumatocysts must remain "air-tight" (Rigg and Swain 1941, Foreman 1976) to avoid leaks and, because compressible gases are susceptible to volumetric change with pressure, must potentially resist rupturing (as gases expand) or buckling (as gases compress; Dromgoole 1981b, Brackenbury et al. 2006) when thalli move through the water column.

Nereocystis thalli are annuals, starting growth in spring (March-April) and ending reproduction in fall (September-October; Rigg 1912, Maxell and Miller 1996). During the spring, young *Nereocystis* thalli can be found growing at maximum depths between 30 and 35 m (Spalding et al. 2003) and grow rapidly toward the surface at a rate of ~14 cm $\cdot$ d^{-1} (Fig. 1; Kain 1987). Like all kelp species, young individuals are composed of a simple holdfast, stipe and blade, and pneumatocysts begin to form within the transition zone between the stipe and the blade ~2 weeks after germination (Nicholson 1970). During development, medullary cells along the transition zone begin to tear, releasing gas internally and creating the pneumatocyst (Dromgoole 1981a). Once pneumatocysts have formed, thalli grow upward and reach the surface in as little as four months (Fig. 1; Duncan 1973). From 30 m deep to the surface, thalli experience a reduction in hydrostatic pressure from 4 atm to 1 atm, that is, 1 atm every 10 m per 10 m (405.3 kPa–101.4 kPa; Fig. 1). As thalli become larger and heavier, with blades that can weigh up to 20 kg in air (Denny et al. 1997), pneumatocysts increase volume, extending into the stipe (see Fig. 1) to increase buoyancy and keep heavy thalli upright. Changes in internal pressure and volume during pneumatocyst development have not been documented, and understanding these changes will help clarify how *Nereocystis* thalli resist mechanical failure and maintain buoyancy across a hydrostatic pressure gradient.

Internal pressure produced by gases is exerted on the inner surface of the pneumatocyst. Since the pneumatocyst is a thick-walled structure (1–10 mm; Foreman 1976), the force differential between the external hydrostatic pressure and the internal pneumatocyst pressure causes material stress. As pneumatocysts move upward through the water column, this force differential could put the pneumatocyst at risk of breaking. Because pneumatocyst walls are rigid and resist volumetric changes that would otherwise equilibrate internal and external pressures (Liggan 2016), wall material must resist applied hydrostatic stress directly, and the geometry, material properties, and deformation of pneumatocysts influence the accumulation of material stress and critical breaking pressure (Dromgoole 1981b).

The ability of pneumatocysts to resist breaking can be assessed by calculating an environmental safety factor (ESF; Johnson and Koehl 1994, Stewart 2006, Koehl et al. 2008). Generally, ESF is the ratio between the breaking stress, the maximum load an object can withstand before breaking, and the working stress, the load it experiences day to day. For example, as ESF approaches 1.0 the structure is performing near capacity, and failure may be imminent; when ESF is 10, the structure is ten-times stronger than it needs to be, and risk is lessened. ESF has previously been applied to *Nereocystis* stipes, to investigate the risk of breaking as the sporophyte increases in size (Johnson and Koehl 1994).

Theoretically, to minimize wall stress and risk of breaking, *Nereocystis* thalli could control the rate of hydrostatic pressure changes by adjusting the rate of stipe growth to slow their ascent. However, stipe elongation rates are rapid (Duncan 1973, Kain 1987), and thalli race to the surface allowing blades to maximize light availability. Instead, we hypothesize that pneumatocysts likely adjust gas production, material properties, or morphology to reduce the risk of breaking during their ascent. For example, pneumatocysts could change the rate of gas production to control internal pressure and maintain a low force differential. Alternatively, if the pressure differential is not maintained, then pneumatocysts could thicken their walls or stiffen their tissues to help resist pressure-induced tissue stress.

In this study, we investigate how internal pressure, morphology, and material properties help pneumatocysts resist mechanical failure as they grow upward through a gradient of hydrostatic pressure in the field. We calculate force differentials experienced by thalli of various sizes to predict when pneumatocysts are at greatest risk of failing. These data allow us to clarify constraints imposed by hydrostatic pressure on developing pneumatocysts and to predict the maximum depth (i.e., pressure) individuals can grow.

MATERIALS AND METHODS

Sample collection. *Nereocystis* thalli ($n = 72$) of varying pneumatocyst volume (3–1,200 cm^3) and varying length (0.15–12 m) were haphazardly collected between April and August 2015 from Ogden Point Breakwater (Victoria, British Columbia, Canada; 48.413542° N, −123.387235° W) with SCUBA from depths up to 9 m. All samples were detached from the substratum at the holdfast so that pneumatocysts were fully intact. Collection depth of the holdfast, day, tidal height (at 0 m chart datum), and time were recorded for each sample. This was used to calculate the depth of each pneumatocyst based on the 0 m tide line. External hydrostatic pressure (P_o) was estimated from pneumatocyst depth as follows:

$$P_o = (\rho g h + P_{atm}) \quad (1)$$

where ρ is the density of seawater (1,025 $kg \cdot m^{-3}$), g is acceleration due to gravity (9.81 $m \cdot s^{-2}$), h is pneumatocyst depth, and P_{atm} is atmospheric pressure.

Pneumatocyst volume was recorded by carving a hole in each pneumatocyst ($n = 72$), filling it with water, then pouring the water into a graduated cylinder three times, taking an average of the three replicates. Pneumatocyst length and width was measured using Image J 64 version 1.49 (National Institutes of Health, Bethesda, MD, USA) by taking photos of each sample with a meter stick. All statistical analyses were conducted using RStudio version 2.11.1 (R Foundation for Statistical Computing; Vienna, Austria).

Measuring internal pressure. Water manometers (diameter: 4–8 mm; length: 20–60 cm) were used in the field to measure internal pressure of pneumatocysts (at the surface) directly after collection (Fig. 2; $n = 64$). Water manometers were attached to pneumatocysts using plastic tubing, a syringe, and a 21 gauge (0.7 mm) needle that was used to puncture pneumatocysts and measure the gas pressure inside. All needles were lubricated with Vaseline to avoid air leaking during the manometer reading. Initial pressure readings were recorded no more than five seconds after the pneumatocysts were punctured. Internal pneumatocyst pressure (P_{pn}) was then calculated by using the dimensions of the manometer and the Ideal Gas Law:

$$\begin{aligned} P_{pn}V_{pn} + P_{mi}V_{mi} &= P_{gauge}V_{gauge} \\ &= P_{gauge}(V_{pn} + V_{mf}) \end{aligned}$$

And so,

$$P_{Pn} = \frac{P_{gauge}(V_{Pn} + V_{mf}) - P_{mi}V_{mi}}{V_{Pn}} \quad (2)$$

where P_{Pn} is the unknown pneumatocyst pressure, P_{gauge} is the pressure reading from the manometer, V_{mf} is the total volume of the manometer from the water line to the needle after the pneumatocyst was punctured, P_{mi} is the pressure of the ambient air in the manometer, V_{mi} is volume of the manometer arm before the pneumatocyst is punctured and V_{Pn} is the volume of the pneumatocyst. Manometer measurement error was calculated as the amount of pressure required to move the water column 1 mm, given the dimensions of the manometer tubing and the difference in volume between manometer and pneumatocyst; error was greatest when pneumatocyst volume was substantially less than manometer volume.

Calculating wall stress. Older pneumatocysts have two different geometries: a cylindrical hollow stipe and a spherical end (see Fig. 1). Because the cylinder portion of the pneumatocyst would experience a different magnitude of material stress than the spherical end, a preliminary study was conducted to determine which portion of the pneumatocyst

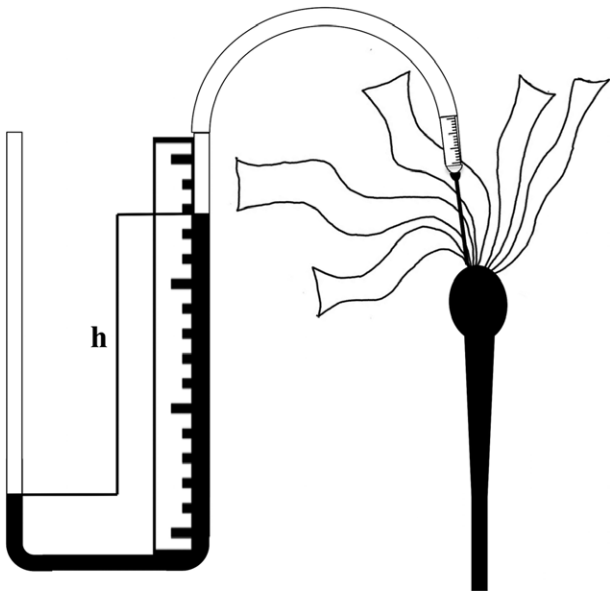

FIG. 2. Diagram of water manometer. Pneumatocysts were punctured using a lubricated syringe needle. Internal pneumatocyst pressure was calculated from the change in water height (h) using eq. 2.

would break first. In the field, we dropped five weighted thalli down to 50 m of seawater, and found that the spherical end of pneumatocysts always broke first. Thus, this study focused on the average wall stress accumulated in the spherical region of the pneumatocyst. Average wall stress in a pneumatocyst at a specific depth was calculated as follows (Fung 1993):

$$\sigma_{avg} = \frac{P_o r_o^2 - P_i r_i^2}{r_o^2 - r_i^2} \quad (3)$$

where σ_{avg} is the average circumferential stress in the pneumatocyst wall, P_o is the external hydrostatic pressure applied to the outer surface of the pneumatocyst wall (calculated from collection depth), P_i is the internal pneumatocyst pressure applied to the inner surface of the pneumatocyst wall (measured by manometer), r_i is the internal pneumatocyst radius (calculated from caliper measurements of pneumatocyst diameter, after subtracting wall thickness), and r_o is the outer pneumatocyst radius (calculated from caliper measurements of pneumatocyst diameter, including wall thickness). Equation 3 takes into consideration that the pneumatocyst is a thick-walled structure and therefore the outer portion of pneumatocyst wall experiences different loads than the inner portion of the pneumatocyst wall. Positive values indicated compressive stresses. All radii and wall thicknesses were measured using calipers to the nearest 1 mm. A linear regression analysis was conducted to determine if material stress changed with pneumatocyst depth.

Compressive modulus. Material properties of pneumatocyst walls were quantified for thalli of varying sizes ($n = 33$; volume = 3–1,200 cm^3) using an Instron 5500R (Model # 1122; Instron Inc., Norwood, MA, USA). Pneumatocysts were cut into circular rings or cubes to measure the elastic modulus (stiffness) of the material. Results between the two shapes were comparable. The Instron was equipped with an 8 × 8 cm block at the base and a 9 × 0.8 cm cross beam atop. All samples were cut to have a height (if ring) and width (if cubed) length no less than 8 mm. Samples were glued onto the top cross beam and the base block using super glue. To ensure the glue did not slip and affect measured stiffness, the adhesion integrity during each test was verified with a high-speed camera (CASIO EX-FH125; Casio America Inc., Dover, NJ, USA). The movement (up or down) of the Instron crossbeam was used to measure strain and these values were compared to real-time measurements analyzed from the video. Each sample was sprayed and hydrated with seawater before each test. Stress was measured by dividing force applied to the sample by its cross-sectional area where it was in contact with the cross-beam. The movement (up or down) of the Instron crossbeam was used to measure strain. All samples were cycled through compression (to −8%) and tension (to 8%) four times to avoid any spuriously high measurements of modulus (i.e., Mullin's effect). Stress-strain curves were linear from −8% to 8% strain (see fig. 7 in Liggan 2016). Young's modulus (initial stiffness) was calculated from the slope of the stress-strain curve during the 4th cycle at 1% compression. A linear regression was used to determine if modulus changed with pneumatocyst volume.

Changes in pneumatocyst geometry. Measured pneumatocyst inner radius (r_i) and wall thickness (t) was used to determine the inner radius to wall thickness ratio (r_i:t), or geometry. Equation 3 takes into consideration that the pneumatocyst is a thick-walled structure and therefore pneumatocyst geometry directly influences average wall stress. Pneumatocyst tissue volume was calculated by estimating the total pneumatocyst volume (tissue and gas space) of a sphere from the pneumatocyst's measured outer radius (r_o) minus the pneumatocyst gas space spherical volume from the pneumatocyst's measured inner radius (r_i).

Environmental safety factor and buckling depth. Calculations suggested that small pneumatocysts (r_i = 0.4–1.0 cm) had elevated wall stress. Therefore small pneumatocysts ($n = 8$) in this size range were collected to test buckling stress and depth. Each thallus was placed into a weighted basket with a SCUBA analogue depth gauge (Scubapro MODEL # 28.019.900) and dropped down to 50 m. A video camera (Go-Pro Hero 3+ silver edition) recorded the sound and depth when each pneumatocyst buckled, detected by an audible "pop." This depth was converted to hydrostatic pressure and internal pressure was averaged across all measured pneumatocysts (80 kPa; shown in Fig. 3), and average buckling stress was then calculated using eq. 3. The ESF of pneumatocysts were then estimated as follows:

$$ESF = \frac{\sigma_{buckle}}{\sigma_{avg}} \quad (4)$$

where σ_{buckle} is the buckling stress of the pneumatocyst wall and σ_{avg} is the wall stress of each pneumatocyst at its collection depth (eq. 3).

RESULTS

Volume and internal pressure. Internal pressure of pneumatocysts did not significantly change with depth (Fig. 3; $F_{1,57} = 2.796$, $P = 0.10$) and was consistently less than atmospheric pressure (101 kPa), ranging from 3 to 100 kPa (Fig. 3). Pneumatocyst internal pressure was less than external hydrostatic pressure at all depths (Fig. 3). Internal pneumatocyst pressure was generally 100–200 kPa less than external hydrostatic pressure below 4 m depth, and 1–50 kPa less than external hydrostatic pressure above 3 m (Fig. 3).

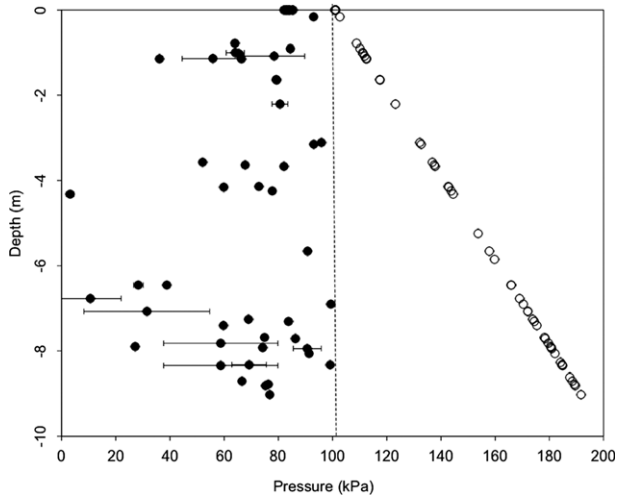

FIG. 3. Internal pneumatocyst pressure (black circles) and hydrostatic pressure (open circles) as functions of pneumatocyst depth. Dotted line represents atmospheric pressure (101 kPa). Error bars represent variation in pressure calculation from 1 mm measurement error on manometer (see Materials and Methods).

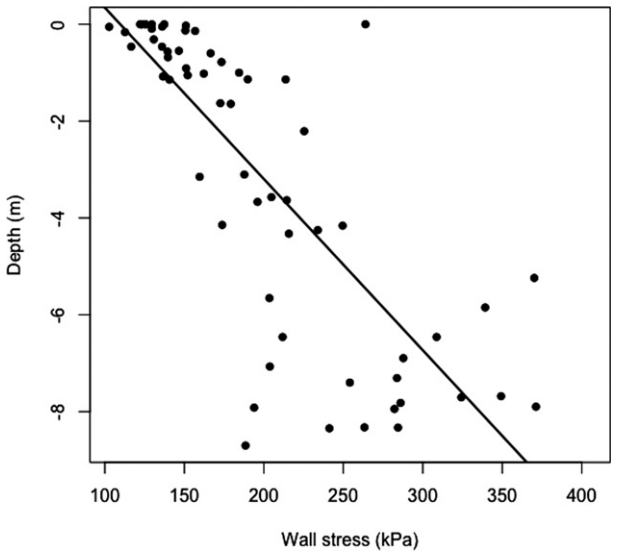

FIG. 4. Wall stresses calculated eq. 3 for pneumatocysts collected from 0 to 9 m depth ($F_{1,60} = 101.2$, $P < 0.001$, $R^2 = 0.62$, $y = 0.03x + 3.05$).

Wall stress, stiffness, and geometry. Pneumatocyst wall stress significantly increased with depth (Fig. 4; $F_{1,60} = 101.2$, $P < 0.001$, $R^2 = 0.62$). Maximum wall stress (375 kPa) was estimated at 8 m depth and minimum wall stress (102 kPa) was estimated at the surface (Fig. 4). The modulus of small pneumatocysts (3–50 cm^3) varied from 0.9 to 10 MPa (Fig. 5). Modulus increased significantly (up to 12 MPa) as pneumatocyst volume increased from 3 to 1,200 cm^3 (Fig. 5; $F_{1,32} = 25.79$, $P < 0.001$, $R^2 = 0.43$). Inner radius increased from 0 cm (before pneumatocyst filled with gas) to 3.5 cm as pneumatocysts grew from 9 m depth to the surface (Fig. 6A). Wall stress was greatest (between 250 and 400 kPa) when pneumatocysts had inner radii between 0.4 and 1.0 cm (Fig. 6B), when tissue volumes were largely unchanged (average volume = 2.3 ± 1.7 cm^3; Fig. 6D), and when ratios of inner radius to wall thickness (r_i:t) varied from 2.8 to 4.0 (Fig. 6C; $F_{1,62} = 84.09$, $P < 0.001$, $R^2 = 0.53$). Pneumatocyst tissue volume increased from 2.3 to 200 cm^3 as pneumatocyst internal radius increased from 1 to 3.5 cm (Fig. 6D).

Buckling stress. Small pneumatocysts (r_i = 0.4–1.0 cm) that were submerged and crushed in the weighted basket had an ESF of 3.4 ± 0.4 (mean + SD; Table 1). Pneumatocysts had an average wall stress between 202 and 287 kPa (Table 1). Buckling stress varied from 786 to 1,032 kPa, and pneumatocysts were observed to buckle on average at 35 ± 4.7 m deep (Table 1).

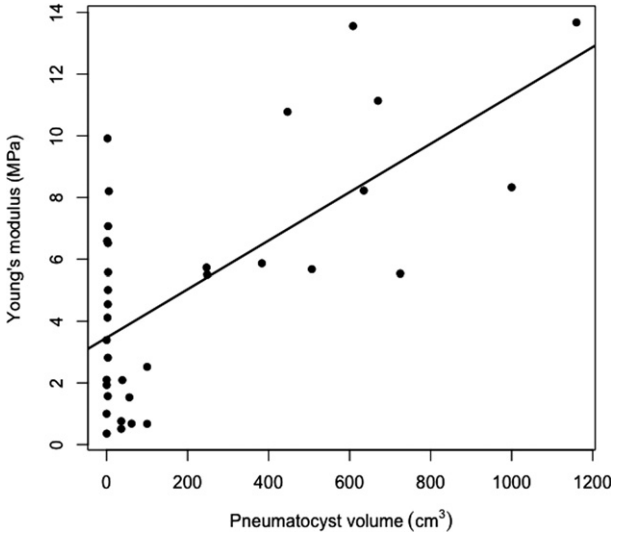

FIG. 5. Young's modulus (material stiffness) as a function of pneumatocyst volumes ($F_{1,32} = 25.79$, $P < 0.001$, $R^2 = 0.43$, $y = 0.01x + 3.5$).

DISCUSSION

Creating a gas-filled cavity that ascends through the water column is a remarkable feat; a single pneumatocyst can experience a change in hydrostatic pressure from 4 atm to 1 atm as the sporophyte grows to increase light interception for photosynthesis. Pneumatocysts endure significant stress from hydrostatic pressure as they ascend toward the surface and, until now, our understanding of how they resist breaking has been limited. Our data suggests that *Nereocystis* thalli do not adjust internal pressure, material properties, nor tissue morphology to survive their ascent but, instead, maintain internal pressures less than atmospheric to ensure that thalli need only resist compression throughout development.

Pneumatocyst internal pressure. Pneumatocysts from all thallus sizes have internal pressures consistently less than ambient hydrostatic pressure and atmospheric pressure at the ocean's surface. Thus, pneumatocysts always experience a positive pressure gradient and are at risk of buckling, not exploding. This strategy ensures that pneumatocyst tissue can specialize in resisting compression and never tension, which would only occur if internal pressure exceeded hydrostatic pressure during development. Other biological materials are known to similarly specialize in either compression (mammalian bone, Reilly and Burstein 1974, cetacean heart valves, Lillie et al. 2013) or tension (mussel byssus, Bell and Gosline 1996, aquatic plants, Etnier and Villani 2007). Future work should examine the histological differences that may exist between *Nereocystis* pneumatocyst tissue, which resists compression, and *Nereocystis* stipe tissue, which is known to resist tension (Johnson and Koehl 1994, Denny et al. 1997, Hale 2001, Denny and Gaylord 2002, Denny and Hale 2003).

Internal pressure did not change significantly or predictably across thalli of different sizes or, presumably, over the lifetime of growing pneumatocysts. This is remarkable as pneumatocyst volume varies from 3 to 1,200 cm^3, yet internal pressure is somehow maintained. Other studies have explored gas production and composition in greater detail (Langdon 1917, Rigg and Swain 1941), in one case demonstrating that the internal pressure in large individuals only changes diurnally by 2 kPa (Liggan 2016). Perhaps even more striking is that juvenile *Nereocystis* have internal pressures consistently less than atmospheric pressure, despite never having been exposed to the surface. We propose that selection may act to ensure that pneumatocyst internal pressure never exceeds hydrostatic or atmospheric pressure; that is, any pneumatocyst with an internal pressure greater than 101 kPa would eventually switch from compression to tension as it ascended through the hydrostatic pressure gradient, causing it to rupture, flood, sink, and become otherwise unviable. Thus, over evolutionary time, *Nereocystis* thalli that maintained internal pressures less than atmospheric pressure may have been more likely to survive and reproduce. Because hydrostatic pressure is always greater than atmospheric pressure, thalli only need to tune their internal pressures according to surface pressure to guarantee that they stay in compression at all depths and locations – a good strategy, unless they happen to grow too deep.

Risk of buckling. Data suggest that young, small pneumatocysts (r_i = 0.4–1.0 cm) are at the greatest risk of buckling. First, because the difference in hydrostatic pressure and internal pressure increases with depth, young pneumatocysts experience the greatest compressive loads. Second, when pneumatocysts initially form, inner radius increases but pneumatocyst walls do not thicken, causing wall

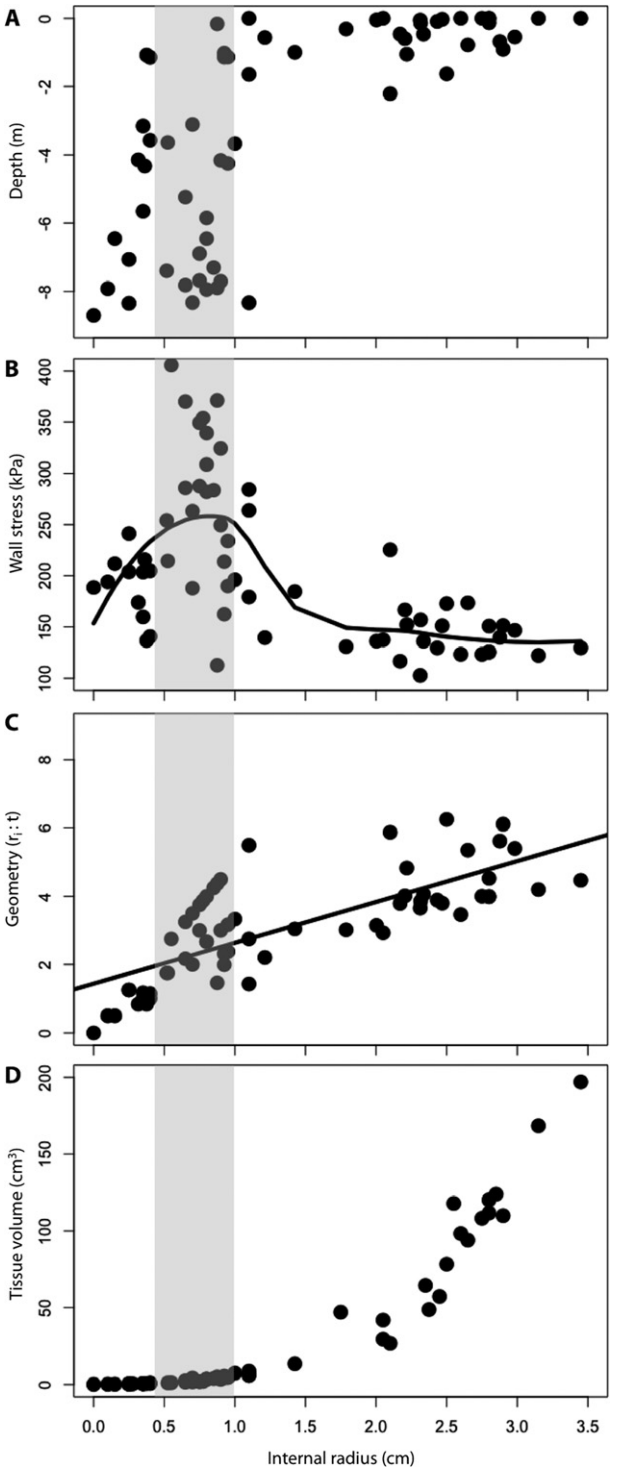

FIG. 6. (A) Collection depth, (B) pneumatocyst wall stress, (C) ratio of internal radius to wall thickness ($F_{1,62}$ = 84.09, $P < 0.001$, R^2 = 0.53, $y = 1.3x + 1.4$), and (D) tissue volume as a function of inner pneumatocyst radius. Data points within the shaded boxes represent young pneumatocysts with an inner radius between 0.4 and 1 cm. Line in part B represents moving average of wall stress and line in part C represents linear regression of geometric ratio against inner radius.

TABLE 1. Collection depth, wall stress, buckling stress, ESF, and buckling depth of 8 young, small pneumatocysts.

Sample	Collection depth (m)	Internal radius (cm)	Wall stress (kPa)	Buckling stress (kPa)	ESF	Buckling depth (m)
1	7.60	0.45	267.38	950.69	3.56	43
2	4.22	0.45	201.86	892.76	4.42	40
3	7.32	0.55	284.56	930.34	3.27	37
4	7.00	0.45	255.45	796.20	3.12	35
5	7.34	0.55	285.11	886.83	3.11	35
6	5.33	0.40	287.26	1,032.13	3.59	32
7	5.89	0.58	258.46	797.76	3.09	30
8	5.44	0.70	245.60	785.94	3.20	30
				Average:	**3.4 ± 0.4**	**35 ± 4.7**

stress to increase: wall stress in young pneumatocysts may be more than double the wall stress estimated in walls of mature pneumatocysts (Fig. 6B). If small pneumatocysts can survive this initial developmental hurdle, wall stress declines and the pressure gradient decreases as thalli mature and ascend through the water column, generally decreasing the overall risk of buckling during the kelp's lifetime.

Theoretically, pneumatocysts could change their geometry or adjust the material stiffness (modulus) of their walls to resist buckling. It has been suggested that a large increase in modulus would be needed to resist breakage as pneumatocyst volume increased (Dromgoole 1981b). However, if pneumatocyst materials were adjusting to resist buckling, modulus would need to be greatest at depth to reduce deformation from elevated wall stress. Contrary to this speculation, the modulus of pneumatocysts is often lowest in young, deep individuals and increases as pneumatocysts age and volume increases. This pattern is consistent with Krumhansl et al. (2015), who noted that kelp tissues tend to get stiffer with age. Thus, according to our data, *Nereocystis* pneumatocysts do not adjust material stiffness to reduce wall stress as they mature. Furthermore, if *Nereocystis* were adjusting pneumatocyst morphology to reduce stress, then r_i:t would be smallest at depth where material wall stress and risk of buckling are greatest. However, smaller pneumatocysts have variable r_i:t ratios from 1:1 to almost 4:1 (i.e., when increased internal volume and constant wall thickness cause elevated wall stress), suggesting that pneumatocysts do not adjust their geometry to reduce wall stress.

Predicting buckling depth. Given that this study found no evidence that pneumatocysts modify geometry, material properties, or internal pressure to offset the risk of buckling, we can predict precisely when pneumatocysts will buckle by estimating buckling stress and depth using measured characteristics. First, data suggest that small pneumatocysts (r_i = 0.4–1.0 cm) are ~3.4 times stronger than they need to be to survive the hydrostatic pressure imposed on them in the field, and hence the young developing pneumatocysts tested in this study were at relatively low risk of buckling. Second, pneumatocysts tested in the weighted basket buckled at ~35 ± 4.7 m depth. Measured buckling depths were remarkably similar to the maximum observed depth of *Nereocystis* (35 m; Spalding et al. 2003). Our calculations suggest that thalli growing at 35 m depth would have an ESF approaching 1 and would be barely capable of tolerating compressive loads. Any increase in hydrostatic pressure at that depth, including big waves passing overhead (Denny and Gaylord 2002), could cause pneumatocysts to buckle. While depth limitation of *Nereocystis* had been attributed previously to light attenuation (Spalding et al. 2003), the present study demonstrates that hydrostatic pressure may also explain the lower limit of *Nereocystis* in the field. Further studies are required to clarify the effects of light and pressure on thallus development and to determine which factor has a greater influence. It is possible that lower limits are predominantly defined by light with thalli adapting to pressure only where light isn't limiting; however, it is equally possible that lower limits are predominantly defined by pressure with thalli adapting to light levels where pressure isn't limiting.

CONCLUSIONS

Nereocystis thalli face biomechanical constraints inflating gas-filled pneumatocysts many meters underwater, which must then ascend through a hydrostatic pressure gradient. Risk of rupture is mitigated not by modifying internal pressure, material properties, or tissue morphology, but by maintaining internal pressures that are consistently less than atmospheric pressure at the surface, ensuring that pneumatocyst walls always experience compressive loads and need not switch from resisting compression to tension during development. Pneumatocysts do not modify material properties or geometry to reduce the risk of buckling; young, small pneumatocysts (r_i = 0.4–1.0 cm) have the greatest wall stresses and are likely at greatest risk of failure due to hydrostatic pressure. However, young pneumatocysts collected during this study were 3.4 times stronger than they needed to be to resist failure in the field, buckling around 35 m depth. Our data suggest that hydrostatic pressure,

not just light attenuation, may help define the lower limit of *Nereocystis* in the field.

This study benefited from the help and support of Dr. Margo Lillie who imparted her knowledge and experience conducting research in the field of biomechanics, particularly with regards to pressure. Fieldwork was tedious and required a cohort of people to collect useful data in a timely manner. Without the SCUBA diving and snorkeling support of Meagan Abele, Samuel Starko, Laura Borden, Bartłomiej Radziej, and Kyra Janot, this study would have been impossible. I am very grateful that the UBC Aqua Society provided endless training, SCUBA tanks, and other resources, which made subtidal collections possible. I would also like to especially thank Sarah Calbick for volunteering many hours collecting data in the lab and field. Finally, this manuscript benefited from the input of Samuel Starko, Jennifer Clark, and Angela Stevenson. All research funds were provided by an NSERC Discovery Grant awarded to PTM.

Bell, E. & Gosline, J. 1996. Mechanical design of mussel byssus: material yield enhances attachment strength. *J. Exp. Biol.* 199:1005–17.

Brackenbury, A. M., Kang, E. J. & Garbary, D. J. 2006. Air pressure regulation in air bladders of *Ascophyllum nodosum* (Fucales, Phaeophyceae). *Algae* 21:245–51.

Charrier, B., Le Bail, A. & de Reviers, B. 2012. Plant Proteus: brown algal morphological plasticity and underlying developmental mechanisms. *Trends Plant Sci.* 17:468–77.

Denny, M. & Gaylord, B. 2002. The mechanics of wave-swept algae. *J. Exp. Biol.* 205:1355–62.

Denny, M., Gaylord, B. P. & Cowen, B. 1997. Flow and flexibility. II. The roles of size and shape in determining wave forces on the bull kelp *Nereocystis luetkeana*. *J. Exp. Biol.* 200:3165–83.

Denny, M. W. & Hale, B. B. 2003. Cyberkelp: an integrative approach to the modeling of flexible organisms. *Philos. T. Roy. Soc. B* 358:1535–42.

Dromgoole, F. 1981a. Form and function of the pneumatocysts of marine algae. I. Variations in the pressure and composition of internal gases. *Bot. Mar.* 24:257–66.

Dromgoole, F. 1981b. Form and function of the pneumatocysts of marine algae. II. Variations in morphology and resistance to hydrostatic pressure. *Bot. Mar.* 24:299–310.

Duncan, M. J. 1973. In situ studies of growth and pigmentation of the phaeophycean *Nereocystis luetkeana*. *Helgoländer Meeresun.* 24:510–25.

Etnier, S. A. & Villani, P. J. 2007. Differences in mechanical and structural properties of surface and aerial petioles of the aquatic plant *Nymphaea odorata* subsp. *tuberosa* (Nymphaeaceae). *Am. J. Bot.* 94:1067–72.

Foreman, R. E. 1976. Physiological aspects of carbon monoxide production by the brown alga *Nereocystis luetkeana*. *Can. J. Bot.* 54:352–60.

Fung, Y. C. 1993. *Biomechanics: Mechanical Properties of Living Tissues*, 2nd edn. Springer Science & Business Media, New York, 357 pp.

Hale, B. 2001. Macroalgal materials: foiling fracture and fatigue from fluid forces. PhD dissertation, Stanford University, 367 pp.

Harder, D. L., Hurd, C. L. & Speck, T. 2006. Comparison of mechanical properties of four large, wave-exposed seaweeds. *Am. J. Bot.* 93:1426–32.

Johnson, A. & Koehl, M. 1994. Maintenance of dynamic strain similarity and environmental stress factor in different flow habitats: thallus allometry and material properties of a giant kelp. *J. Exp. Biol.* 195:381–410.

Kain, J. M. 1987. Patterns of relative growth in *Nereocystis luetkeana* (Phaeophyta). *J. Phyc.* 23:181–7.

Koehl, M. A. R. 1999. Ecological biomechanics of benthic organisms: life history, mechanical design and temporal patterns of mechanical stress. *J. Exp. Biol.* 202:3469–76.

Koehl, M. A. R., Silk, W. K., Liang, H. & Mahadevan, L. 2008. How kelp produce blade shapes suited to different flow regimes: a new wrinkle. *Integr. Comp. Biol.* 48:834–51.

Koehl, M. A. R. & Wainwright, S. A. 1977. Mechanical adaptations of a giant kelp. *Limnol. Oceanog.* 22:1067–71.

Krumhansl, K. A., Demes, K. W., Carrington, E. & Harley, C. D. 2015. Divergent growth strategies between red algae and kelps influence biomechanical properties. *Am. J. Bot.* 102:1938–44.

Lane, C. E., Mayes, C., Druehl, L. D. & Saunders, G. W. 2006. A multi-gene molecular investigation of the kelp (Laminariales, Phaeophyceae) supports substantial taxonomic re-organization. *J. Phyc.* 42:493–512.

Langdon, S. C. 1917. Carbon monoxide, occurrence free in kelp (*Nereocystis luetkeana*). *J. Am. Chem. Soc.* 39:149–56.

Liggan, L. 2016. Under pressure: biomechanics of buoyancy in Bull Kelp (*Nereocystis luetkeana*). MS dissertation, University of British Columbia, Vancouver, 78 pp.

Lillie, M. A., Piscitelli, M. A., Vogl, A. W., Gosline, J. M. & Shadwick, R. E. 2013. Cardiovascular design in fin whales: high-stiffness arteries protect against adverse pressure gradients at depth. *J. Exp. Biol.* 216:2548–63.

Maxell, B. & Miller, K. 1996. Demographic studies of the annual kelps *Nereocystis luetkeana* and *Costaria costata* (Laminariales, Phaeophyta) in Puget Sound, Washington. *Bot. Mar.* 39:479–89.

Nicholson, N. L. 1970. Field studies on the giant kelp *Nereocystis*. *J. Phycol.* 6:177–82.

Reilly, D. T. & Burstein, A. H. 1974. The mechanical properties of cortical bone. *J. Bone Joint Surg.* 56:1001–22.

Rigg, G. B. 1912. Notes on the ecology and economic importance of *Nereocystis luetkeana*: a contribution from the Puget Sound marine station. *The Plant World* 15:83–92.

Rigg, G. B. & Swain, L. A. 1941. Pressure-composition relationships of the gas in the marine brown alga, *Nereocystis luetkeana*. *Plant Physiol.* 16:361.

Spalding, H., Foster, M. S. & Heine, J. N. 2003. Composition distribution, and abundance of deep-water (>30 m) macroalgae in central California. *J. Phyc.* 39:273–84.

Springer, Y., Hays, C., Carr, M. & Mackey, M. M. 2007. Ecology and management of the Bull Kelp, *Nereocystis luetkeana*. Lenfest Ocean Program report, 53 pp.

Starko, S. & Martone, P. T. 2016. Evidence of an evolutionary-developmental trade-off between drag avoidance and tolerance strategies in wave-swept intertidal kelps (Laminariales, Phaeophyceae). *J. Phycol.* 52:54–63.

Stewart, H. L. 2006. Ontogenetic changes in buoyancy, breaking strength, extensibility, and reproductive investment in a drifting macroalga *Turbinaria ornata* (Phaeophyta). *J. Phycol.* 42:43–50.

Thiel, M. & Gutow, L. 2005. The ecology of rafting in the marine environment. I. The floating substrata. *Oceanogr. Mar Biol.* 42:181–264.

Utter, B. & Denny, M. 1996. Wave-induced forces on the giant kelp *Macrocystis pyrifera* (Agardh): field test of a computational model. *J. Exp. Biol.* 199:2645–54.

Yoon, H. S., Lee, J. Y., Boo, S. M. & Bhattacharya, D. 2001. Phylogeny of Alariaceae, Laminariaceae, and Lessoniaceae (Phaeophyceae) based on plastid-encoded RuBisCo spacer and nuclear-encoded ITS sequence comparisons. *Mol. Phylogenet. Evol.* 21:231–43.